International Journal of Cardiology 276 (2019) 1–7

Contents lists available at ScienceDirect

International Journal of Cardiology

journal homepage: www.elsevier.com/locate/ijcard

Discrepant myocardial microvascular perfusion and mechanics after acute myocardial infarction: Characterization of the "Tako-tsubo effect" with real-time myocardial perfusion contrast echocardiograph☆

Qiong Qiu [a,b], Mahmoud Abdelghany [a], Rogin Subedi [a], Ernest Scalzetti [c], David Feiglin [c], Jingfeng Wang [b,*], Kan Liu [a,*]

[a] Division of Cardiology, State University of New York, Upstate Medical University, Syracuse, NY 13202, United States of America
[b] Division of Cardiology, Sun Yat-sen Memorial Hospital of Sun Yat-sen University, Guangzhou 510120, China
[c] Department of Radiology, State University of New York, Upstate Medical University, Syracuse, NY 13202, United States of America

ARTICLE INFO

Article history:
Received 20 April 2018
Received in revised form 11 August 2018
Accepted 28 September 2018
Available online 4 October 2018

Keywords:
Myocardial infarction
Myocardial perfusion contrast echocardiography
Heart failure
Cardiogenic shock
Tako-tsubo syndrome
Stress-induced cardiomyopathy

ABSTRACT

Background: In patients with acute anterior myocardial infarction (MI), sometimes an "apical ballooning" contractile dysfunction pattern that exceeds factual myocardial injury is identified in the ventriculography and bedside echocardiography. The hemodynamic consequences/sequela of this "Tako-tsobu effect" has not been well delineated. Of note, this anatomic imaging finding often misleads frontline physicians who assume reciprocal causation of persistent cardiac pump failure and ventricular pressure overload.

Methods and results: Using real-time myocardial perfusion contrast echocardiography (MCE), we investigated myocardial (microvascular) perfusion in 60 patients after acute MI and coronary revascularization. Twenty-eight percent of the studied patients showed significantly mismatched myocardial perfusion and contractile defects. In these patients, an integrated imaging assessment with coronary angiography/ventriculography, deformation echocardiography, and MCE proved that the myocardial mechanic abnormalities significantly exceeded the defected perfusion areas. Compared with 72% of the patients without perfusion-contractility mismatch, apparently worse systolic functions (left ventricular ejection, wall motion score, and systolic longitudinal strain) in these patients did not change diastolic ventricular filling pressures (E/E′ and E/A) or hemodynamic consequences/adverse events. Both systolic and diastolic functions in patients with perfusion-contractility mismatch appeared to be comparable with those in patients with Tako-tsubo syndrome.

Conclusions: Real-time MCE identifies discrepant myocardial microvascular perfusion and mechanics in patients with acute MI. The "Tako-tsubo effect" in patients with perfusion-contractility mismatch does not cause diastolic filling pressure change or worse hemodynamic consequence/cardiac event.

1. Introduction

Although prompt coronary revascularization has reduced myocardial infarction (MI)-associated mechanical complications [1,2], acute MI-induced ventricular dilation sometimes continues, resulting in an assumption of reciprocal causation of persistent pump failure and ventricular pressure overload [3–6]. A real-time imaging approach to instantaneously evaluate factual myocardial injury and to discover discordant ventricular contractile function and filling pressure [4,7–9] would help preload titration and avoid adverse hemodynamic consequences during post-MI management.

Myocardial perfusion contrast echocardiography (MCE) has assumed an increasingly greater role in assessing myocardial microvascular pathology and subclinical ischemia [10–12]. Assessment of the gradual refill of microbubbles into coronary microcirculation allows detection of inconsistent myocardial blood circulation from conductive to microvascular vessels [13]. Integrated with simultaneous functional/Doppler assessments [7], MCE often leads to a better understanding of the real-time changes of myocardial perfusion, ventricular function, and hemodynamics.

We investigated microvascular myocardial perfusion with MCE in 60 patients within 48 h after acute MI and percutaneous coronary intervention (PCI). An essential portion of these patients showed discrepant microvascular myocardial perfusion and ventricular contractile defect. An integrated imaging approach with coronary angiography/

☆ All the authors take responsibility for all aspects of the reliability and freedom from bias of the data presented and their discussed interpretation.

* Correspondence to: Kan, Liu, Division of Cardiology/Heart and Vascular Center, University of Iowa, Iowa City, IA 52242, United States of America, and Jingfeng Wang, Department of Cardiology, Sun Yat-sen Memorial Hospital, Sun Yat-sen University, Guangzhou, China.
E-mail addresses: Kan-Liu@uiowa.edu (K. Liu), dr_wjf@vip.163.com (J. Wang).

https://doi.org/10.1016/j.ijcard.2018.09.114
0167-5273/

ventriculography, deformation echocardiography, and MCE further demonstrated that the myocardial mechanic abnormalities significantly exceeded the defected perfusion area. Paradoxically, compared with the patients without perfusion-contractility mismatch, apparently worse ventricular systolic function in these patients did not significantly worsen diastolic function (filling pressure) or hemodynamics. Their systolic and diastolic functions were comparable to those in patients with Tako-tsubo syndrome (TTS).

2. Methods

Informed consent was obtained from each patient. The study protocol conformed to the ethical guidelines of the 1975 Declaration of Helsinki as reflected in a priori approval by the institutional research board of the Human Subjects Committee of the State University of New York (SUNY) Upstate Medical University.

2.1. Patients

From 01/01/2012 to 02/28/2016, we completed MCE in 60 patients admitted to the coronary care unit (CCU) of SUNY Upstate Medical University Hospital, following acute MI and percutaneous coronary intervention (PCI). PCI was performed according to the updated European Society of Cardiology/American College of Cardiology guidelines [14]. Transthoracic echocardiography (TTE) with MCE was performed within 48 h after PCI/CCU admission. Patients were excluded if they had primary valvular disorders, significant pulmonary arterial hypertension, or motion of ventricular segments associated with infarct-related artery that could not be accurately determined in either left ventriculography (LVG) or TTE.

Based on the results from coronary angiograms (CAG), LVG, two-dimensional (2D) and speckle tracking echocardiograms, we defined "perfusion-contractility mismatch" as the following: 1) mismatched LVG and CAG: ventricular dilation involved the myocardial regions not supplied by culprit coronary arteries; 2) mismatched echocardiogram and CAG: ventricular wall motion abnormalities involved the myocardial regions not supplied by culprit coronary arteries; 3) ventricular wall motion abnormalities beyond the culprit coronary artery territories (Fig. 1 A) normalized within 3 months after PCI. The studied patients who met all of the above criteria were assigned to the "mismatched MI (mis-MI)" group. All of the others were assigned to the "matched MI (mat-MI)" group. We compared clinical presentations, coronary artery anatomies, systolic and diastolic ventricular functions, inpatient hemodynamic consequences, and short-term (30 days) cardiovascular outcomes.

Meanwhile, we completed a systematic search of the computerized database Epic Electronic Medical Record at SUNY Upstate University Hospital and identified 67 consecutive TTS patients from 01/01/2012 through 02/28/2016. The diagnostic criteria for TTS followed the updated diagnostic guideline [15,16]: (1) Characteristic left ventricular (LV) segment wall motion abnormalities, including apical ballooning and mid-ventricular akinesis/dyskinesis on the initial LVG or TTE; (2) ST segment or T-wave abnormalities on electrocardiogram (ECG) and increases in blood concentrations of cardiac troponin T/creatine kinase MB; (3) No significant culprit coronary artery stenosis revealed; (4) If there were contraindications for an immediate cardiac catheterization, the diagnosis would be valid based on follow-up TTE documenting complete normalization of cardiac systolic function/segmental wall motion without cardiovascular revascularization, and CAG, stress echocardiography or cardiovascular single-photon emission-computed tomography to rule out the existence of culprit coronary artery stenosis.

2.2. 2D Doppler echocardiography

TTE was performed with standard techniques using GE Vivid E9 machine (GE Healthcare, Vingmed Ultrasound A/S, Norway). A 3.5-MHz phased-array transducer was used for standard comprehensive 2D Doppler echocardiography. LV ejection fraction (LVEF) was calculated by biplane Simpson's method from apical 4- and 2-chamber views. Blood flow velocities across the mitral valve (E and A velocities) and mitral annulus (myocardial) velocity (e′) were measured during early diastole. Right ventricular ejection fraction (RVEF) was calculated by the single-plane Simpson's method from the apical 4-chamber view. Tei-index, right ventricular (RV) fractional area change (FAC), and tricuspid annular plane systolic excursion (TAPSE) were performed following the updated guidelines of the Society of Echocardiography [17]. A standard 17-segment ventricular model [17] was used for segmental wall motion analysis. Regional wall motion was semi-quantitatively evaluated using wall motion score (WMS) and defined as 4 grades (1 = normal, 2 = hypokinetic, 3 = akinetic, 4 = dyskinetic/aneurismal). The segments were further grouped as basal (6 segments), middle (6 segments), and apical (5 segments), and WMS of each group was calculated by averaging the WMS of these segments [17]. The WMS index (WMSI) was calculated by the sum of all segments score and divided by the total number of segments.

2.3. Myocardial deformation/systolic longitudinal strain assessment

2D grayscale images were acquired in the standard apical views. Only images with frame rates >40 frames/s were selected for reliable analysis. All images were stored digitally for subsequent offline analysis. Speckle tracking analysis automatically tracked myocardial motion throughout the cardiac cycle and allowed a rapid generation of regional myocardial strain curves. We traced the endocardial border at the end of ventricular systole and adjusted the width of the ventricular walls to include the entire myocardium. Built-in software automatically accepted segments with good tracking quality and rejected segments with poor tracking quality. Finally, an automated function imaging based on speckle tracking analysis integrated the quantitative data of ventricular peak systolic longitudinal strain into a standard 17-segment model with a "bull's-eye" figure, helping detect both regional and global ventricular dysfunction. The 17 LV segments were grouped as basal (6), middle (6), and apical (5) segments for statistical analysis, and the strain value of each group was calculated by averaging the peak systolic longitudinal strain [18,19]. Strain analyses were performed by 2 cardiologists (QQ and KL) independently who were blinded to the patients' clinical and biochemical data.

2.4. Myocardial contrast echocardiography

After activating contrast preset, the focus was adjusted on the mitral valve. The mechanical index was turned to <0.2 with minimum gain to reduce tissue background. The contrast (Optison, GE Healthcare) was injected with 0.3 mL intravenously, followed by 3–5 mL of 0.9% normal saline. After LV opacification, depletion-replenishment technique was performed: "flash" impulse (mechanical index = 1.3) to clear the contrast in the myocardium with visible destruction, then apical 4-, 3-, and 2-chamber views were recorded respectively under lower mechanical index (<0.2) for 10 cardiac cycles. Myocardial opacification was visually assessed by semi-quantitative score based on the change and peak of myocardial signal intensity as follows: 1 = absent (no opacification throughout replenishment), 2 = reduced (partial or reduced opacification at peak or reduced replenish rate), 3 = normal (homogeneous opacification and normal replenish rate). Reduced replenish rate was defined as myocardial opacification occurred after 3 heartbeats since flashing. Meanwhile, basal, middle, and apical perfusion scores were calculated separately. The perfusion score index was used to quantify whole ventricular perfusion and was calculated by the sums of all perfusion scores divided by the total number of segments. For quantitative analysis, the sample volume was placed and modified on each segment. The time-intensity curve was generated automatically. After fitting to a monoexponential function [$Y = A\,(1 - e^{-bt})$], plateau signal intensity (A) was calculated to measure myocardial blood volume [20]. If it did not fit the formula, the segment was rejected for the next analysis. MCE analyses were performed by 2 cardiologists (QQ and KL) independently who were blinded to the patients' clinical and biochemical data.

2.5. Cardiac catheterization with CAG and LVG

Cardiac catheterizations with selective coronary angiography were performed with standard techniques [14]. LVG was performed with a pigtail catheter. Results were recorded in both standard reports and digital imaging. LV pressures and aortic systolic and diastolic pressure were recorded. Angiographic LV volumes were computed with standard methods. Based on the coronary artery anatomies, all of the ventricular segments were divided into culprit and non-culprit artery territories [21]. Two interventional cardiologists who were unaware of the clinical and coronary angiography findings evaluated images independently. Both the anatomic features and Gensini score were recorded. According to culprit artery location and dominant and major side-branches circulations, the segments were divided into culprit/non-culprit artery-supplied areas based on the 17-segment model [21].

2.6. Follow-up data

Follow up data were obtained through reviewing electronic records, including coronary artery disease (CAD) risk factors, clinical presentations, blood pressure, cardiac enzymes, and medical therapy. Follow-up was completed within 30 days after MI by using mailed questionnaires, telephone interviews, a review of medical records, and the Social Security Agency Death Index. The major adverse cardiac events (MACE) were recorded, including cardiac death, MI, stroke, heart failure (HF) requiring admission, symptomatic arrhythmia requiring admission, or pacemaker implantation.

2.7. Statistics

Normal distributed quantitative data were expressed as mean value ± standard deviation (SD) and compared using Student's *t*-test or one-way analysis of variance (ANOVA). Otherwise, median (25th–75th) was used and compared with the Mann-Whitney *U* test or Kruskal-Wallis test. Categorical data were presented as absolute values and percentages, and compared using χ^2 or Fisher's exact test. Correlations were calculated using the Spearman correlation coefficient test. SPSS software package for Windows 21 (IBM Corporation, New York, USA) was used for all statistical analysis. The significance was established at 2-tailed $P < 0.05$.

3. Results

3.1. Demographic/clinical characteristics

Among 60 patients who underwent MCE, 17 had mis-MI and 43 had mat-MI. The demographic/clinical data were summarized in Table 1.

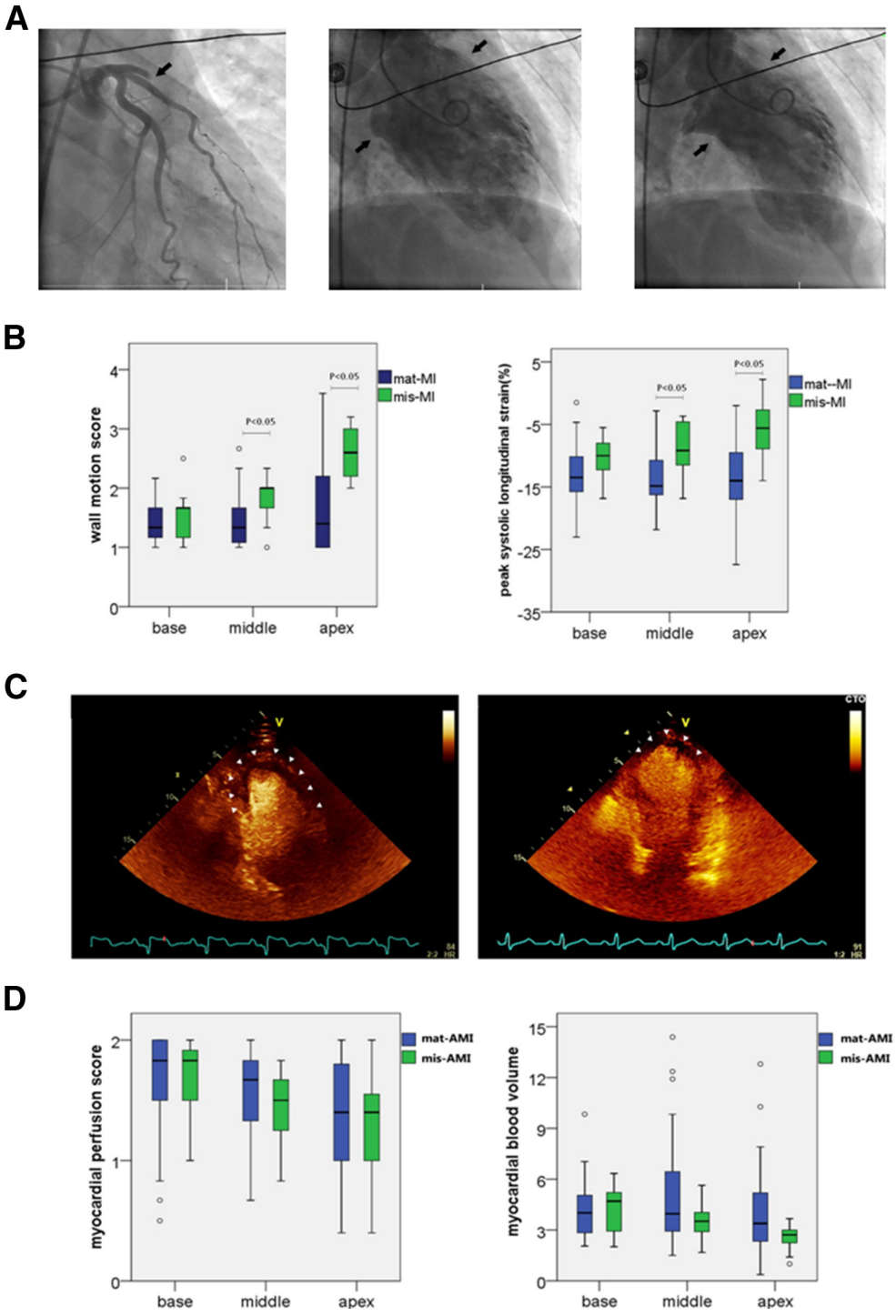

Fig. 1. A: The "apical ballooning" ventricular contractile pattern in a patient with an acute myocardial infarction (MI) caused by left anterior descending artery stenosis: The myocardial mechanic abnormalities are beyond the territory of the culprit coronary artery. B: More myocardial mechanic abnormalities in the middle and apical left ventricle (LV) in mis-MI patients from wall motion score (left) and myocardial deformation (right, peak systolic longitudinal strain). C: The systolic contractile dysfunction correlated well with the microvascular perfusion defect in a mat-MI patient (left), but not in a mis-MI patient (right); D: There are no difference in microvascular myocardial perfusion between mis-MI and mat-MI patients (left, myocardial perfusion score index; right, myocardial blood volume).

Mean age of mis-MI patients was 58.5 years old and 41.2% of them were female. Ninety-four percent of mis-MI patients had angina, and 70.6% did not have prior MI. Between mis-MI and mat-MI patients, there were no significant differences in CAD risk factors, including hypertension, diabetes mellitus, hyperlipidemia, smoking history, and psychiatric disorders. There were no significant differences in previous medication of angiotensin-converting enzyme inhibitor/angiotensin receptor blocker and beta-blockers. The time intervals from the onset of angina to PCI were not significantly different between mis-MI and mat-MI patients. For coronary artery anatomy (Table 1), more mis-MI patients had left anterior descending artery (LAD) as the culprit vessel. Wrapped LAD and pre-existing collateral circulations were similar in mis-MI and mat-MI patients. Fewer mis-MI patients had multi-vessel diseases. Gensini scores were similar between the 2 groups.

Table 1
Demographic and clinical characteristics in mis-MI and mat-MI patients.

Variable	mis-MI (n = 17)	mat-MI (n = 43)	*P*-value
Demographic data			
Age (years)	58.5 ± 12.9	58.1 ± 13.5	0.197
Female, n (%)	7 (41.2)	9 (20.9)	0.110
Primary AMI, n (%)	12 (70.6)	30 (69.8)	0.950
Chest pain n (%)	16 (94.1)	38 (88.4)	0.504
Risk factors and medication history			
Hypertension, n (%)	11 (64.7)	32 (74.4)	0.452
Diabetes, n (%)	5 (29.4)	14 (32.6)	0.813
Hyperlipidemia, n (%)	10 (58.8)	27 (62.8)	0.776
Smoking, n (%)	9 (52.9)	18 (41.9)	0.437
Psychiatric disorder[a]	2 (11.8)	7 (16.3)	0.501
ACEI/ARB, n (%)	4 (23.5)	21 (48.8)	0.073
β-Blocker	3 (17.6)	12 (27.9)	0.317
Laboratory measures			
Peak CK-MB (IU/L)[b]	154.2 (37.0–467.1)	64.5 (24.9–238.9)	0.181
Peak cTnT (ng/mL)[b]	4.7 (1.7–15.0)	2.5 (0.7–5.0)	0.110
Coronary angiography			
Angina to PCI time (hour)[b]	3.3 (2.3–11.1)	3.3 (2.2–14.5)	0.914
LAD as culprit artery, n (%)	14 (82.4)	24 (55.8)	0.049
Proximal LAD occlusion, n (%)	8 (47.1)	16 (37.2)	0.339
LAD wrap around, n (%)	8 (47.1)	16 (37.2)	0.339
Collateral arteries, n (%)	4 (23.5)	7 (16.3)	0.513
Multivessel disease, n (%)[c]	5 (29.4)	25 (58.1)	0.045
Gensini score[b]	55.0 (20.0–80.0)	40.0 (31.0–80.0)	0.780
Systolic and diastolic function in echocardiography			
LVEF (%)	44.0 ± 12.0	53.7 ± 15.0	0.020
E/A[a]	1.0 (0.7–1.6)	1.1 (0.9–1.5)	0.339
E/e′[a]	9.1 (7.8–11.8)	8.3 (7.1–12.4)	0.487
Tei-index	0.62 ± 0.22	0.42 ± 0.22	0.007
FAC (%)	42.7 ± 12.7	47.5 ± 10.7	0.185
TAPSE (cm/s)	22.5 ± 4.1	22.5 ± 3.9	0.979
Hemodynamic consequences			
Pulmonary edema, n (%)	2 (11.8)	9 (20.9)	0.336
Hypotension, n (%)[e]	6 (35.5)	10 (23.3)	0.352
End-organ hypoperfusion, n (%)[d]	4 (23.5)	12 (27.9)	0.501
Killip grade >1 n (%)	9 (52.9)	24 (55.8)	0.840
Adverse cardiac events			
30-day hospital readmission, n (%)	2 (11.8)	4 (9.3)	0.551
MACE (30 days), n (%)	3 (17.6)	8 (18.6)	0.191

a, psychiatric disorders include affective disorder, anxiety disorder, reaction to severe stress or adjustment disorder; b, with stenosis >50%; c, expressed as median (25th–75th); d, systolic blood pressure <90 mm Hg; e: end-organ hypoperfusion was defined as altered mental status, cold and clammy skin, oliguria (urine output <0.5 mL/kg/h for 2 consecutive hours, or a serum creatinine rise >80 mol/L within 24 h), increased serum lactate (>2 mmol/L). ACEI, angiotensin-converting enzyme inhibitor; ARB, angiotensin-receptor blocker; CK-MB, creatine kinase–muscle/brain; cTnT, cardiac troponin T; E/A, ratio of early (E) to late (A) diastolic mitral valve velocity; E/e′, mitral valve E velocity divided by mitral annular e′ velocity; FAC, fractional area change; LAD, left anterior descending coronary artery; LVEF, left ventricular ejection fraction; MACEs, major adverse cardiac events, including cardiac death, recurrent myocardial infarction, stroke, heart failure requiring admission, malignant arrhythmia; MI, myocardial infarction; mat-MI, MI patients with matched perfusion-contractility; mis-MI, MI patients with mismatched perfusion contractility; PCI, percutaneous coronary intervention; TAPSE, tricuspid annular plane systolic excursion.

3.2. Ventricular wall motion and myocardial deformation abnormality

Compared with mat-MI patients, mis-MI patients had more LV segments with contractile dysfunction (62.3% vs. 35.3%, $P < 0.001$). Their WMSI scores were significantly higher (1.9 ± 0.3 vs. 1.5 ± 0.5, $P < 0.001$), mainly due to worse contractile dysfunction in the middle and apical LV segments (Fig. 1B). Global systolic longitudinal strain (−8.6 ± 4.2% vs. −13.6 ± 4.9%, $P = 0.07$) were significantly impaired in mis-MI patients.

In mat-MI patients, angiographically projected dysfunctional myocardial regions correlated well with both echocardiographically measured dysfunctional ventricular segments ($r = 0.353$, $P = 0.027$) and WMSI ($r = 0.389$, $P = 0.014$). In mis-MI patients, these correlations no longer existed. More than half of the hypokinetic (in both 2D and strain measurements) LV segments were not supplied by "culprit" coronary arteries.

3.3. Myocardial perfusion

There was no significant difference in myocardial microvascular perfusion between mis-MI and mat-MI patients, evaluated with either semi-quantitative (myocardial perfusion score index: 1.47 ± 0.31 vs. 1.54 ± 1.47, $P > 0.05$) or quantitative (myocardial blood volume: 3.44 ± 0.62 vs. 4.65 ± 2.73, $P > 0.05$) methods. Also, there were no significant differences of the regional (basal, middle, or apical) myocardial perfusion abnormality between these 2 groups (Fig. 1D). In mat-MI patients, the segmental wall motion abnormalities correlated well with myocardial microvascular perfusion defects ($r = -0.157$, $P < 0.001$). In contrast, in mis-MI patients, up to 38.0% hypokinetic ventricular segments had normal myocardial perfusion with no correlation between the segmental WMS and myocardial microvascular perfusion (Fig. 1C). Similarly, myocardial deformation abnormalities correlated well with microvascular perfusion defects in the mat-MI group ($r = 0.159$, $P < 0.05$), but not in the mis-MI group.

3.4. Ventricular systolic/diastolic dysfunction and hemodynamic consequences

In mis-MI patients, LVEFs were significantly lower (44.0 ± 12.0% vs. 53.7 ± 15.0%, $P = 0.02$), and Tei-index was significantly impaired (0.62 ± 0.22 vs. 0.42 ± 0.22, $P < 0.01$). Nonetheless, no significant differences were found in E/A ratio or E/e′ ratio between these 2 groups. Also, there were no significant differences in RV functional parameters between these 2 groups, including FAC and TAPSE (Table 1).

There was no significant difference in the clinical or imaging evidence of decompensated HF between mis-MI and mat-MI patients. Also, there was no significant difference in symptoms/signs or laboratory evidence of the cardiac shock between the 2 groups. Their Killip classifications and median hospitalization time were similar. The hospital re-admission rates and MACEs were similar between both groups within 30 days after discharge (Table 1).

3.5. Comparison of functional/hemodynamic features between patients with mis-MI and TTS

An "apical ballooning" ventricular contractile pattern occurred in most of mis-MI patients (Fig. 2). Their abnormal WMS increased from basal to apical ventricles, and absolute values of myocardial strains descended from basal to apical ventricles, both of which were comparable to the findings in patients with TTS (Fig. 2). Moreover, there were no significant differences in LV and RV systolic/diastolic function parameters, including LVEF, Tei-index, E/A, E/e′, global myocardial deformation, FAC, and TAPSE between mis-MI and TTS patients (Table 2).

4. Discussion

The present study identified discrepant myocardial mechanic dysfunction and microvascular perfusion defect in a substantial portion of patients with acute MI. Using an integrated imaging approach, we demonstrated that apparently worse ventricular systolic function in these patients did not result in significant change in diastolic function (filling pressure) or adverse hemodynamic consequences/events. The patients with the perfusion-contractility mismatch displayed comparable systolic and diastolic function features with patients with TTS.

"Myocardial stunning" describes a delayed recovery of myocardial contractile function after a successful coronary revascularization, which has been delineated to be limited within the culprit coronary

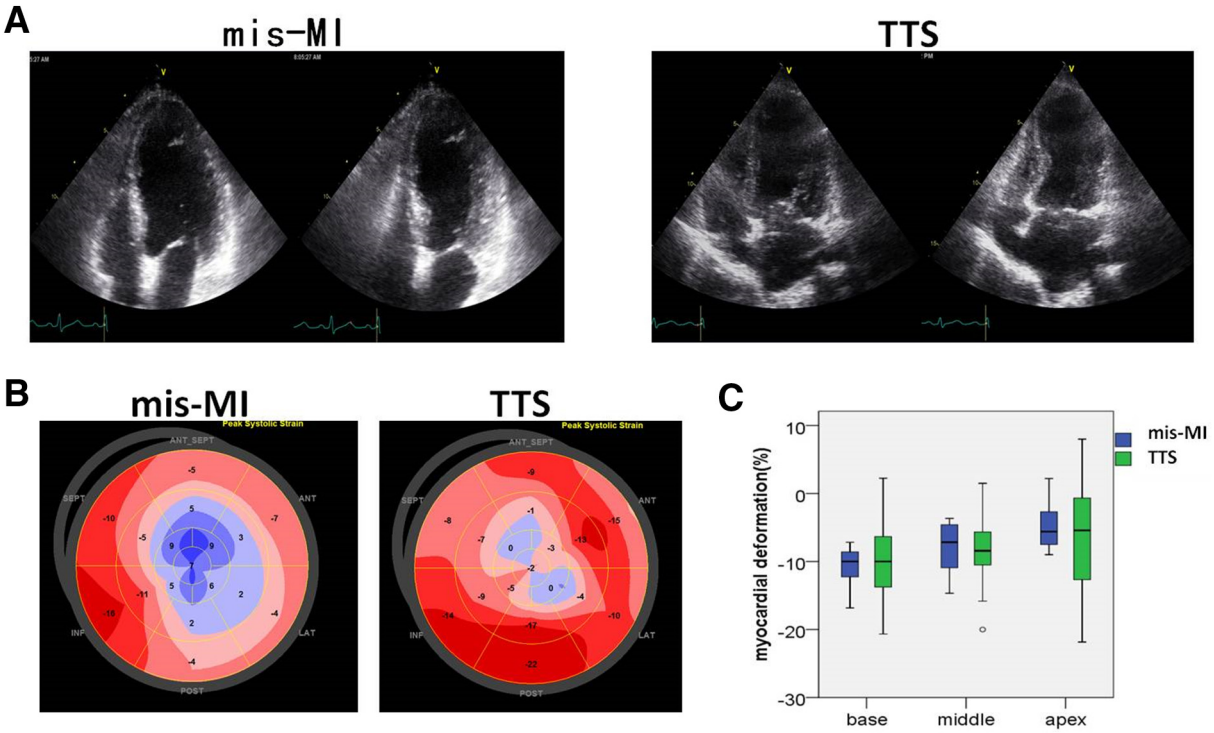

Fig. 2. Comparable ventricular functional and mechanic features in mis-MI and Tako-tsubo syndrome (TTS) patients. A: The "apical ballooning" ventricular contractile patterns in both mis-MI (left) and TTS (right) patients in the 4-chamber view echocardiography; B: Comparable basal to apical myocardial strain gradients in mis-MI (left) and TTS (right) patients in the speckle tracking echocardiography; C: There are no significant differences in basal, middle, and apical strain measurements (peak systolic longitudinal strain) between mis-MI and TTS patients.

artery territory [22,23]. The previous imaging studies on "myocardial stunning", including integrative approach with cardiac positron emission tomography and magnetic resonance imaging [24,25], showed that both edema and suppressed metabolic status coexisted in the hypokinetic myocardium surrounding the MI [26]. These "peri-infarct" abnormalities were attributed to the presence of microvascular perfusion pathology, including microvascular obstruction, and intramyocardial hemorrhage [27,28]. In the present study, we integrated MCE with both invasive and non-invasive imaging technique, and demonstrated that myocardial mechanic abnormalities during the acute stage of MI indeed exceed not only the territories of the culprit coronary arteries, but also the microvascular perfusion defects.

While coronary angiography primarily delineates epicardial coronary structure, MCE assesses the "real" blood flow perfusion into coronary microcirculation, which is able to uncover inconsistent myocardial blood circulations from conductive to microvascular vessels [29]. The microbubbles from MCE remain exclusively inside the intravascular space, and their presence denotes the effective microvascular perfusion status. The contrast intensity also correlates well with regional capillary blood volume and cellular integrity, and predicts myocardial viability and long-term ventricular remodeling [29–31]. The safety of echocardiography contrast has been previously investigated in large multicenter trials [32], including critically ill patients [33,34] and patients after AMI [35]. No side effects (headache, flushing back pain, or anaphylaxis reaction) occurred in our studied patients receiving MCE within 48 h after AMI and revascularization.

In the present study, mis-MI patients exhibited broader and worse ventricular wall motion abnormalities, which were not limited within the territories of either culprit coronary arteries or microvascular perfusion defects (Fig. 1C and D). To exclude myocardial tethering and translational effect, and demarcate the "actual" wall motion impairment [36], we evaluated myocardial deformation with strain/speckle tracking echocardiography. In mis-MI patients, the myocardial regions with impaired myocardial deformations were still significantly beyond the myocardium with defected microvascular perfusion. Therefore, in contrast to previous findings (24–28), we conclude that microvascular perfusion pathology was unlikely the sole mechanism responsible for these ventricular contractile dysfunctions.

Although the clinical manifestation of TTS often mimics that of an acute anterior wall MI, TTS is postulated to have completely different etiology, pathophysiology, and prognosis [15]. However, an "apical ballooning" contractile distribution pattern has frequently been identified in the patients with acute anterior MI [37]. In our previous investigations with 2D [38] and strain echocardiography [39], we identified the similarity in the ventricular morphology, particularly the distribution patterns of the contractile dysfunction between TTS and certain groups of MI patients. With invasive and noninvasive techniques, the present study extends similar finding to diastolic function/hemodynamics.

Table 2
Systolic and diastolic function in mis-MI and Tako-tsubo syndrome patients.

Variable	mis-MI (n = 17)	TTS (n = 66)	*P*-value
LVEF (%)	44.0 ± 12.0	40.5 ± 6.8	0.265
Global longitudinal strain[a]	−8.6 ± 1.2%	−8.2 ± 4.3%	0.743
E/A[b]	1.0 (0.7–1.6)	1.1 (0.7–1.4)	0.838
E/e′[b]	9.1(7.8–11.8)	11.2 (9.2–14.2)	0.055
Tei-index	0.62 ± 0.22	0.73 ± 0.27	0.135
RVEDA (cm^2)	13.9 ± 3.9	16.0 ± 5.4	0.132
RVESA (cm^2)	7.7 ± 3.9	8.3 ± 3.2	0.541
RVFAC (%)	42.7 ± 12.7	48.1 ± 9.3	0.071
TAPSE (cm/s)	22.5 ± 4.1	21.9 ± 3.8	0.617

a, available in 11 mis-MI and 50 TTC patients; b, expressed as median (25th–75th). E/A, ratio of early (E) to late (A) diastolic mitral valve velocity; E/e′, mitral valve E velocity divided by mitral annular e′ velocity; RVFAC, right ventricular fractional area change; LVEF, left ventricular ejection fraction; RVEDA, right ventricular end diastolic area; RVESA, right ventricular end systolic area; TAPSE, tricuspid annular plane systolic excursion; TTS, Tako-tsubo syndrome.

TTS is typically precipitated by acute emotional or psychological stressors, with excessive sympathetic stimulation playing an essential role in its pathogenesis [15,40]. During acute MI, pain and other stressors can stimulate central and autonomic nervous systems and increase bioavailability of cortisol and circulating catecholamines [41,42], which affect the myocardium supported by both culprit and non-culprit coronary arteries [43,44]. Due to higher density of β-adrenergic receptors and proportion of β2 receptors linked to Gi than Gs proteins in the ventricular apex [45,46], wall motion impairment can predominantly present in the apical and middle segments of the ventricle, forming a characteristic "apical ballooning" ventricular geometric change. Just like TTS, this "Tako-tsubo effect" neither indicates factual cardiac pump failure [47] nor worsens hemodynamics [48,49]. Instead, it likely represents a universal pathophysiological response in an acutely injured heart, and shares certain common underlying mechanism with TTS.

Despite abrupt ventricular morphological changes and apparently severe ventricular dysfunction, most TTS patients maintain hemodynamic stability and benign clinical course [15]. Molecular research revealed that TTS was likely mediated by a cardioprotective signal transduction pathway, which evolved as a self-protective strategy [46]. Our clinical investigations [38,39,47] also support the self-protective roles of TTS in maintaining hemodynamics. In the patients with "Tako-tsubo effect", in our study, although different imaging parameters such as LVEF, WMSI and global myocardial strain all indicating significantly depressed systolic function, their diastolic function and filling pressures [50] were not significantly affected (Table 1). Consequently, adverse cardiac events or hemodynamic consequences, including cardiogenic shocks and decompensated heart failure, did not increase.

The post-MI ventricular morphological abnormalities may not correlate with factual cardiac pump failure. The volume management should not be based spontaneously on the assumption of reciprocal causation of pump failure and ventricular pressure overload. In the past, acute MI-induced cardiac pump failure was frequently accompanied by severe vasoconstriction. In the recent years, patients with CAD had often already received outpatient vasodilators, including angiotensin-converting enzyme inhibitors and β-blockers, and their vasoconstriction was less severe during acute MI. Low peripheral resistance and low preload could coexist, resulting in intolerance of vasodilators, circulatory aggravation, and even hemodynamic instability [7,51]. With the guidance of real-time parametric imaging, timely titrating the ventricular preload helps prevent hemodynamic consequences/events and fulfills the goal of personalized medicine in post-MI management.

4.1. Limitations

There are several limitations in the present study. First, MI and TTS are both highly dynamic and time-variant processes. Their real-time ventricular contractile functions and filling pressures can vary significantly at different time points. The comparison at a single point during two dyssynchronous temporal courses might not accurately reflect the changes during patients' entire progressive courses. Secondly, as a pilot project in patients with acute MI, which required comprehensive invasive and non-invasive assessments, including MCE, a relative small number of patients were recruited in our study. This could cause selection bias and undermine statistical analysis. Finally, current MCE protocols, particularly the quantification methods, are not standardized and need validation in future multi-centered prospective trials.

Disclosures

This study was supported by GE Investigor Initiated Trial (to KL) and a National Natural Science Foundation of China Grant (to QQ, No. 8170020989).

Conflict of interest

None.

References

[1] M. Tisminetzky, D.D. McManus, J.M. Gore, et al., 30-year trends in patient characteristics, treatment practices, and long-term outcomes of adults aged 35 to 54 years hospitalized with acute myocardial infarction, Am. J. Cardiol. 113 (7) (2014) 1137–1141.
[2] D.D. McManus, M. Chinali, J.S. Saczynski, et al., 30-year trends in heart failure in patients hospitalized with acute myocardial infarction, Am. J. Cardiol. 107 (3) (2011) 353–359.
[3] S. Jha, S.D. Flamm, D.H. Kwon, Revascularization in heart failure in the post-STICH era, Curr. Heart Fail. Rep. 10 (4) (2013) 365–372.
[4] N. Kronas, J.C. Kubitz, S. Forkl, G.I. Kemming, A.E. Goetz, D.A. Reuter, Functional hemodynamic parameters do not reflect volume responsiveness in the immediate phase after acute myocardial ischemia and reperfusion, J. Cardiothorac. Vasc. Anesth. 25 (5) (2011) 780–783.
[5] G. Greenberg, A. Assali, H. Assa-Vaknin, et al., Outcome of patients presenting with ST elevation myocardial infarct and cardiogenic shock: a contemporary single center's experience, Cardiology 122 (2) (2012) 83–88.
[6] A. Reyentovich, M.H. Barghash, J.S. Hochman, Management of refractory cardiogenic shock, Nat. Rev. Cardiol. 13 (8) (2016) 481–492.
[7] J. Lei, A.S. Dhamoon, J. Wang, M. Iannuzzi, K. Liu, Walking the tightrope: using quantitative Doppler echocardiography to optimize ventricular filling pressures in patients hospitalized for acute heart failure, Eur. Heart J. Acute Cardiovasc. Care. 5 (2) (2016) 130–140.
[8] K. Bendjelid, Five recurrent misconceptions regarding cardiogenic shock management, Cardiol. Rev. 22 (5) (2014) 241–245.
[9] I. Danad, J. Szymonifka, J.W.R. Twisk, et al., Diagnostic performance of cardiac imaging methods to diagnose ischaemia-causing coronary artery disease when directly compared with fractional flow reserve as a reference standard: a meta-analysis, Eur. Heart J. w95 (2016).
[10] T.R. Porter, S. Abdelmoneim, J.T. Belcik, et al., Guidelines for the cardiac sonographer in the performance of contrast echocardiography: a focused update from the American Society of Echocardiography, J. Am. Soc. Echocardiogr. 27 (8) (2014) 797–810.
[11] T.R. Porter, F. Xie, Contrast echocardiography: latest developments and clinical utility, Curr. Cardiol. Rep. 17 (3) (2015) 569.
[12] R. Senior, A. Moreo, N. Gaibazzi, et al., Comparison of sulfur hexafluoride microbubble (SonoVue)-enhanced myocardial contrast echocardiography with gated single-photon emission computed tomography for detection of significant coronary artery disease, J. Am. Coll. Cardiol. 62 (15) (2013) 1353–1361.
[13] T.R. Porter, L.M. Smith, J.F. Wu, et al., Patient outcome following 2 different stress imaging approaches a prospective randomized comparison, J. Am. Coll. Cardiol. 61 (24) (2013) 2446–2455.
[14] G.N. Levine, E.R. Bates, J.C. Blankenship, et al., 2015 ACC/AHA/SCAI Focused Update on Primary Percutaneous Coronary Intervention for Patients with ST-Elevation Myocardial Infarction: an update of the 2011 ACCF/AHA/SCAI Guideline for Percutaneous Coronary Intervention and the 2013 ACCF/AHA Guideline for the Management of ST-Elevation Myocardial Infarction, J. Am. Coll. Cardiol. 67 (10) (2016) 1235–1250.
[15] A.R. Lyon, E. Bossone, B. Schneider, et al., Current state of knowledge on Takotsubo syndrome: a position statement from the Taskforce on Takotsubo Syndrome of the Heart Failure Association of the European Society of Cardiology, Eur. J. Heart Fail. 18 (1) (2016) 8–27.
[16] A. Prasad, A. Lerman, C.S. Rihal, Apical ballooning syndrome (Tako-Tsubo or stress cardiomyopathy): a mimic of acute myocardial infarction, Am. Heart J. 155 (3) (2008) 408–417.
[17] R.M. Lang, L.P. Badano, V. Mor-Avi, et al., Recommendations for cardiac chamber quantification by echocardiography in adults: an update from the American Society of Echocardiography and the European Association of Cardiovascular Imaging, J. Am. Soc. Echocardiogr. 28 (1) (2015) 1–39.
[18] C.L. Hung, A. Verma, H. Uno, et al., Longitudinal and circumferential strain rate, left ventricular remodeling, and prognosis after myocardial infarction, J. Am. Coll. Cardiol. 56 (22) (2010) 1812–1822.
[19] K. Liu, R. Krone, Evaluation of coronary steal in myocardium supplied by coronary collaterals: the role of speckle tracking analysis in resting and stress echocardiography, Echocardiography. 30 (9) (2013) 1111–1117.
[20] S.S. Abdelmoneim, M.W. Martinez, S.V. Mankad, et al., Resting qualitative and quantitative myocardial contrast echocardiography to predict cardiac events in patients with acute myocardial infarction and percutaneous revascularization, Heart Vessel. 30 (1) (2015) 45–55.
[21] J.T. Lee, R.E. Ideker, K.A. Reimer, Myocardial infarct size and location in relation to the coronary vascular bed at risk in man, Circulation 64 (3) (1981) 526–534.
[22] R. Bolli, Mechanism of myocardial "stunning", Circulation 82 (3) (1990) 723–738.
[23] P.G. Camici, S.K. Prasad, O.E. Rimoldi, Stunning, hibernation, and assessment of myocardial viability, Circulation 117 (1) (2008) 103–114.
[24] H. Bulluck, S.K. White, G.M. Fröhlich, et al., Quantifying the area at risk in reperfused ST-segment–elevation myocardial infarction patients using hybrid cardiac positron emission tomography–magnetic resonance imaging clinical perspective, Circ. Cardiovasc. Imaging. 9 (3) (2016), e3900.
[25] F. Nensa, T. Poeppel, E. Tezgah, et al., Integrated FDG PET/MR imaging for the assessment of myocardial salvage in reperfused acute myocardial infarction, Radiology 276 (2) (2015) 400–407.

[26] J.T. Ortiz-Perez, S.N. Meyers, D.C. Lee, et al., Angiographic estimates of myocardium at risk during acute myocardial infarction: validation study using cardiac magnetic resonance imaging, Eur. Heart J. 28 (14) (2007) 1750–1758.
[27] S.K. White, D.J. Hausenloy, J.C. Moon, Imaging the myocardial microcirculation post-myocardial infarction, Curr. Heart Fail. Rep. 9 (4) (2012) 282–292.
[28] R.P. Betgem, G.A. de Waard, R. Nijveldt, A.M. Beek, J. Escaned, N. van Royen, Intramyocardial haemorrhage after acute myocardial infarction, Nat. Rev. Cardiol. 12 (3) (2015) 156–167.
[29] L. Galiuto, B. Garramone, A. Scara, et al., The extent of microvascular damage during myocardial contrast echocardiography is superior to other known indexes of post-infarct reperfusion in predicting left ventricular remodeling: results of the multicenter AMICI study, J. Am. Coll. Cardiol. 51 (5) (2008) 552–559.
[30] G. Dwivedi, R. Janardhanan, S.A. Hayat, J.M. Swinburn, R. Senior, Prognostic value of myocardial viability detected by myocardial contrast echocardiography early after acute myocardial infarction, J. Am. Coll. Cardiol. 50 (4) (2007) 327–334.
[31] T.M. Khumri, S. Nayyar, M. Idupulapati, et al., Usefulness of myocardial contrast echocardiography in predicting late mortality in patients with anterior wall acute myocardial infarction, Am. J. Cardiol. 98 (9) (2006) 1150–1155.
[32] S.S. Abdelmoneim, M. Bernier, C.G. Scott, et al., Safety of contrast agent use during stress echocardiography in patients with elevated right ventricular systolic pressure: a cohort study, Circ. Cardiovasc. Imaging. 3 (3) (2010) 240–248.
[33] M.L. Main, M.G. Hibberd, A. Ryan, T.J. Lowe, P. Miller, G. Bhat, Acute mortality in critically ill patients undergoing echocardiography with or without an ultrasound contrast agent, JACC Cardiovasc. Imaging 7 (1) (2014) 40–48.
[34] A. Putrino, D.G. Platts, Contrast echocardiography in acutely unwell patients, J. Am. Soc. Echocardiogr. 28 (7) (2015) 844.
[35] F.A. Flachskampf, M. Schmid, C. Rost, S. Achenbach, A.N. DeMaria, W.G. Daniel, Cardiac imaging after myocardial infarction, Eur. Heart J. 32 (3) (2011) 272–283.
[36] V. Mor-Avi, R.M. Lang, L.P. Badano, et al., Current and evolving echocardiographic techniques for the quantitative evaluation of cardiac mechanics: ASE/EAE consensus statement on methodology and indications, J. Am. Soc. Echocardiogr. 24 (3) (2011) 277–313.
[37] T. Chao, J. Lindsay, S. Collins, et al., Can acute occlusion of the left anterior descending coronary artery produce a typical “takotsubo” left ventricular contraction pattern? Am. J. Cardiol. 104 (2) (2009) 202–204.
[38] A. Singh, J. Lei, H. Kozman, J. Wang, K. Liu, “Reverse McConnell's Sign”: a unique right ventricular mechanical and functional feature in Tako-Tsubo cardiomyopathy, Circulation 130 (2014), A13894.
[39] J. Lei, Z.X. Sun, L.C. Lyu, R.G. Green, E. Scalzetti, M. McGrath, D. Feiglin, J. Wang, K. Liu, Mechanical interventricular dependency supports hemodynamics in Tako-tsubo cardiomyopathy, J. Thorac. Dis. 10 (5) (2018) 3027–3038.
[40] C. Templin, J.R. Ghadri, J. Diekmann, et al., Clinical features and outcomes of Takotsubo (stress) cardiomyopathy, N. Engl. J. Med. 373 (10) (2015) 929–938.
[41] Y. Yu, Z.H. Zhang, S.G. Wei, J. Serrats, R.M. Weiss, R.B. Felder, Brain perivascular macrophages and the sympathetic response to inflammation in rats after myocardial infarction, Hypertension 55 (3) (2010) 652–659.
[42] A. Gimelli, P.G. Masci, R. Liga, et al., Regional heterogeneity in cardiac sympathetic innervation in acute myocardial infarction: relationship with myocardial oedema on magnetic resonance, Eur. J. Nucl. Med. Mol. Imaging 41 (9) (2014) 1692–1694.
[43] F. Ferrara, C. Baldi, M. Malinconico, et al., Takotsubo cardiomyopathy after acute myocardial infarction: an unusual case of possible association, Eur. Heart J. Acute Cardiovasc. Care. 5 (2) (2016) 171–176.
[44] J.A. Parker, A.L. Amerini, R. Autschbach, J.W. Spillner, Takotsubo cardiomyopathy with concurrent multivessel obstructive coronary artery disease: proposition for a new clinical entity and first case surgical experience, Interact. Cardiovasc. Thorac. Surg. 14 (1) (2012) 108–109.
[45] Y. Shao, B. Redfors, T.M. Scharin, et al., Novel rat model reveals important roles of beta-adrenoreceptors in stress-induced cardiomyopathy, Int. J. Cardiol. 168 (3) (2013) 1943–1950.
[46] H. Paur, P.T. Wright, M.B. Sikkel, et al., High levels of circulating epinephrine trigger apical cardiodepression in a beta2-adrenergic receptor/Gi-dependent manner: a new model of Takotsubo cardiomyopathy, Circulation 126 (6) (2012) 697–706.
[47] Z. Sun, P. Singh, T. Wei, H. Kozman, K. Liu, Is the heart really stressed out of energy? JACC Cardiovasc. Imaging 9 (5) (2016) 633–635.
[48] K. Liu, Z. Sun, T. Wei, “Reverse McConnell's Sign”: interpreting interventricular hemodynamic dependency and guiding the management of acute heart failure during Takotsubo cardiomyopathy, Clin. Med. Insights Cardiol. 9 (Suppl. 1) (2015) 33–40.
[49] K. Liu, R.J. Krone, What truly causes the adverse outcome in Tako-Tsubo cardiomyopathy? JACC Cardiovasc. Imaging 7 (7) (2014) 742–743.
[50] G.S. Hillis, J.E. Møller, P.A. Pellikka, et al., Noninvasive estimation of left ventricular filling pressure by e/e′ is a powerful predictor of survival after acute myocardial infarction, J. Am. Coll. Cardiol. 43 (3) (2004) 360–367.
[51] C.W. Yancy, M. Jessup, B. Bozkurt, et al., 2017 ACC/AHA/HFSA Focused Update of the 2013 ACCF/AHA Guideline for the Management of Heart Failure: a report of the American College of Cardiology/American Heart Association Task Force on Clinical Practice Guidelines and the Heart Failure Society of America, Circulation 136 (6) (2017) e137–e161.